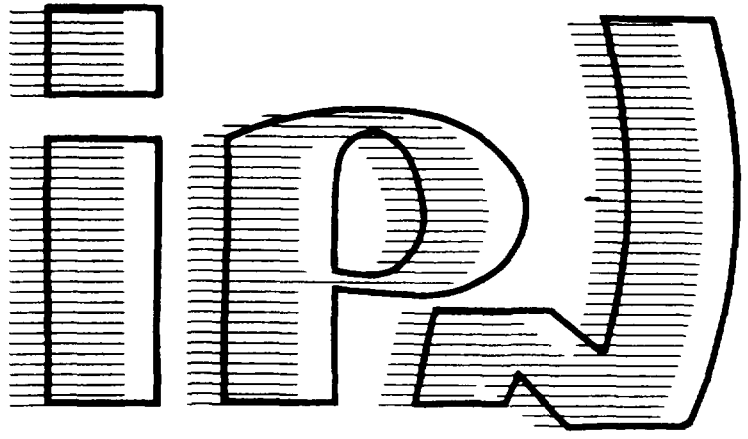




FR9700750

Gestion INIS
Doc. enreg. le : 12/3/95
N° TRN :
Destination : I,I+D,D



IPNO - DRE 95-16

**LIFETIME MEASUREMENTS BY DELAYED
COINCIDENCES WITH AND WITHOUT A COMPLETE
KNOWLEDGE OF THE PROMPT CURVE.
APPLICATION TO LEVELS IN 184IR AND 185,187PT.**

**J. Oms, M.C. Abreu, C. Bourgeois, F. Bragança Gil
and the ISOCELE Collaboration**

2

IPNO - DRE 95-16

**LIFETIME MEASUREMENTS BY DELAYED
COINCIDENCES WITH AND WITHOUT A COMPLETE
KNOWLEDGE OF THE PROMPT CURVE.
APPLICATION TO LEVELS IN ^{184}Ir AND $^{185,187}\text{Pt}$.**

**J. Oms, M.C. Abreu, C. Bourgeois, F. Bragança Gil
and the ISOCELE Collaboration**

LIFETIME MEASUREMENTS BY DELAYED COINCIDENCES WITH AND WITHOUT A COMPLETE KNOWLEDGE OF THE PROMPT CURVE. APPLICATION TO LEVELS IN ^{184}Ir AND $^{185,187}\text{Pt}$

J.OMS^a, M.C.ABREU^b, C.BOURGEOIS^a, F.BRAGANÇA GIL^b
and the ISOCELE Collaboration

a) Institut de Physique Nucléaire, 91406 Orsay, France

b) Departamento de Física, Faculdade de Ciências da Universidade de Lisboa,
1700 Lisboa Codex, Portugal

Submitted to Nuclear Instruments and Methods

ABSTRACT. A method is described which enables one to deduce a range of possible values for the lifetime of a nuclear level when the delayed coincidence curve is experimentally given and the prompt curve is known only through some of its features. The method still applies when a prompt contribution is present. Experimental data in ^{184}Ir are analyzed, and yield $T_{1/2}(293.3 \text{ keV}) = 1.1(3) \text{ ns}$, $T_{1/2}(70.7) \leq 180 \text{ ps}$. The method is also used to discuss results obtained with an experimental prompt curve in ^{185}Pt . [~~$T_{1/2}(200) = 728(20) \text{ ps}$ and ^{187}Pt [$T_{1/2}(260) = 163(6) \text{ ps}$, $T_{1/2}(180.8) = 1.68(4) \text{ ns}$].~~

1. Introduction

The delayed-coincidence method is the most widely used for measuring the lifetime of nuclear states ranging from a few picoseconds to a few nanoseconds, and even longer.

Unless the lifetime τ to be measured is long relative to the time resolution of the apparatus, in which case the "slope method" may be used, this method requires the knowledge of the "prompt" curve to yield the τ value. This necessity may be a severe experimental requirement, especially as the prompt curve should ideally be registered under exactly the same energy and counting rates conditions as the delayed curve. The prompt curve is often obtained with a separate calibration source. It then means a constraint which is all the more felt when nuclei with a short half-life are studied, as such experiments entail mechanical complications besides activity variations.

To avoid this constraint self-calibration methods have been used [1-3]. More recently methods have been developed which take advantage of the possibilities brought by the simultaneous multi-analysis of several transitions. Some of these measurements assume the prompt curve to be gaussian-shaped, with an adjustable width. In the generalized centroid-shift method [4-6] the reference is often given by some transitions present in the spectrum, which are regarded as very fast and are used for an interpolation. Similarly the β - γ - $\gamma(t)$ method relies, to some extent, on internal calibrations [7-9]. In this connection it may be mentioned that delayed coincidences containing two decay constants could in principle be analyzed without a prompt curve [10].

In the present work life-time measurements have been performed in transitional neutron-deficient ^{184}Ir and $^{185,187}\text{Pt}$ nuclei by delayed electron- γ or electron-electron coincidences which involve mostly low-energy transitions and for which the experimental device used is particularly well-suited. They have been analyzed by a method which may give upper and, eventually, lower limits for the τ value. When a prompt curve is available this method, combined with a conventional analysis, provides a test for the consistency of the results.

2. Deconvoluting the delayed curve

If $P(t)$ represents the time distribution of the prompt curve, then [11] the delayed time distribution (or delayed curve) $F(t)$ is given by

$$F(t) = \int_0^{\infty} P(t-t') \cdot \exp(-t'/\tau) \cdot dt' \quad (1)$$

An equivalent [12] relation is

$$P(t) = \frac{dF}{dt} + \frac{F}{\tau} \quad (2)$$

with $P(t)$ normalized to 1.

Eq.(2) shows that, if $F(t)$ is given, a function $P(t)$ corresponds, from a purely mathematical viewpoint, to any value of τ . From a physical viewpoint, if neither $P(t)$ nor τ are known, one nevertheless may have some general indications about $P(t)$. The most general is that $P(t)$ starts with a zero value for a given t , then increases with t , reaches a single maximum and drops to zero again. Some other indications may arise from an experimental study of the properties of the coincidence set-up (cf. e.g. sect.5.1). Putting together all these constraints and regarding τ as a variable, one may get an upper and eventually a lower bound for the physically possible τ values.

Eq.(1) does not hold any more when a prompt contribution, which could originate from scattered electrons or Compton photons, is superimposed to the delayed curve. The observed delayed curve may then be written as

$$F(t) = A \cdot P(t) + \int_0^{\infty} P(t-t') \cdot \exp(-t'/\tau) \cdot dt' \quad (3)$$

where A is a constant and A/τ represents the ratio of the total numbers of prompt to delayed events.

The time distribution of true delayed coincidences is

$$\varphi(t) = F(t) - A \cdot P(t) \quad (4)$$

Owing to eq.(2), $P(t)$ satisfies

$$P(t) = \frac{d\varphi}{dt} + \frac{\varphi}{\tau} \quad (5)$$

which may be rewritten, taking eq.(4) into account, as

$$P(t) (1 + (A/\tau)) + A \cdot \frac{dP}{dt} = \frac{dF}{dt} + \frac{F(t)}{\tau} \quad (6)$$

Thus, for an experimentally known $F(t)$ distribution, the prompt distribution $P(t)$ corresponding to a given (A, τ) couple is solution of a differential equation.

The foregoing relations assume that the transition which triggers the "start" of the TAC precedes the other one. When the contrary case was encountered in this work, the analysis was performed on the curve obtained by reversing the direction of the t -axis in order for these relations to remain valid.

3. Numerical techniques

The computation of $P(t)$ from eq.(2) is straightforward but, for practical purposes, the function $F(t)$ has to be smoothed before computing the derivative $dF(t)/dt$. Rather than using an involved and bias-generating mathematical procedure, it was found more convenient to operate graphically by drawing a smooth curve between the experimental points: the validity of the method is fully justified by the insensitivity of the results, and even more of the conclusions, to small variations of the curve compatible with the experimental data. The time was expressed as a channel number, and the function $F(t)$ was linearly interpolated between the integer values of t .

Eq.(6) is solved by a 4th order Runge-Kutta method (e.g. ref.13). For this purpose it is written under the form

$$P'(t) = f[t, P(t)] = (1/A) \cdot \left[\frac{dF}{dt} + \frac{F(t)}{\tau} - P(t) \left(1 + \frac{A}{\tau} \right) \right] \quad (7)$$

thus defining a function $f(t, y)$ with $y = P(t)$, and the initial condition chosen is $P(0) = 0$.

An integration step h is taken, along with the following definitions

$$t_n = nh, \quad n=0, 1, 2, \dots \quad (8)$$

$$\phi(t, y, h) = (k_1 + 2k_2 + 2k_3 + k_4) / 6 \quad (9)$$

with

$$k_1 = f(t, y) \quad (10)$$

$$k_2 = f[t + (h/2), y + (hk_1/2)] \quad (11)$$

$$k_3 = f[t + (h/2), y + (hk_2/2)] \quad (12)$$

$$k_4 = f(t+h, y+hk_3) \quad (13)$$

The method then assumes that

$$P(t_{n+1}) = P(t_n) + h \phi [t_n, P(t_n), h] \quad (14)$$

As $\partial F / \partial y = -(A^{-1} + \tau^{-1})$ may be regarded as a continuous and bounded function, a theorem states that the method is stable [13], i.e. little sensitive to small errors occurring during the calculation. Looking further into the matter, it is easy to show analytically that a small computational error occurring at a given step has an effect which decreases exponentially in the following steps. But the ultimate test for the validity of the method is the possibility to correctly reproduce the experimental $F(t)$ function by a numerical integration (eq.3) in which $P(t)$ is used. In all the numerous test cases the reproduction obtained was well within the experimental uncertainties and almost indistinguishable from the original function when a step $h=0.01$ channel was used for both the resolution of the differential equation and the integration. This step was routinely used in the following computations. It is likely that a larger step would also have been possible in most cases, but the procedure is so fast that no appreciable computer time would have been saved.

4. Experimental techniques

The activity was produced at the Orsay Synchrocyclotron and separated by the on-line mass-separator ISOCELE [14]. It was collected on small Al discs, which were 1.5mm thick for $e^- - \gamma$ coincidences and 0.75 μm for $e^- - e^-$. After collection the source was automatically moved to the counting position, while another disc was brought in. Used sources were also carried away by the device. The collection and counting times could be set separately in order to optimize the activity of the desired nuclide. The counting position was at the focus of a double magnetic-lens β -spectrometer [15]. The focused electrons were detected with a plastic NE111 scintillator associated with an XP2020 photomultiplier. For $e^- - \gamma$ coincidences one of the lenses was removed and the photons ($E_\gamma > 500$ keV) detected by a scintillator distant 1cm from the source. A fast-slow coincidence circuit was used.

5. Lifetime measurements in ^{184}Ir

Levels in ^{184}Ir were fed by the EC/ β^+ decay [16,17] of ^{184}Pt , which has a 17.3 min half-life. The activity was produced with 200 MeV protons and a

gold target by the $^{197}\text{Au} (p, 14n) ^{184}\text{Hg}$ reaction, followed by an EC/β^+ decay chain.

5.1 Lifetime of the 293.3 keV 2^+ level

A first attempt to measure this lifetime was done by $e^- - \gamma$ coincidences, focusing the electron spectrometer on the L67.6 conversion line (fig.1) and using a ^{60}Co source to get the prompt curve. Two separate measurements were performed. The data were analyzed with the MULPAC program [18] which, and this is important, allows for a prompt contribution. The results were $T_{1/2} = 1.4 \pm 0.2 \text{ ns}$ and $T_{1/2} = 1.06 \pm 0.13 \text{ ns}$ (statistical uncertainties).

However, considering that the L67.6 peaks are strongly admixed with the L70.7 and L58.4 lines and that the statistics was insufficient to reveal the eventual presence of two lifetimes, another measurement was carried out by coincidences between the L67.6 and L49.4 conversion lines. The result is shown in fig.2.

A lifetime appears on the left side of the curve (fig.2), which shows that, in agreement with the level scheme, the 67.6 keV transition follows the 49.4 keV one. This lifetime is however too short to be safely determined by the slope method, and no prompt curve is available for a conventional deconvolution to be performed. So the analysis was done following the method described in sect. 2 and 3 and conducted in the $[\tau, A/\tau]$ plane (fig.3).

A first condition to be fulfilled by the $P(t)$ curve is that it should have no negative values and no secondary maxima. This, through a systematic scan, eliminates the hatched zone of the plane. More information can be extracted from the delayed curve by observing that it exhibits a strong change in the slope slightly above half the maximum height, whereas experience tells that - with the device used - nothing similar happens with a prompt curve when the energy of the detected electrons is well defined. With this remark in mind, and taking into account the general properties of the $P(t) \rightarrow F(t)$ transform defined by eq. (1) or (3), the delayed curve appears as the superposition of a prompt curve (or a slightly delayed one) and a pure delayed curve (free from any prompt contribution). Defining the "asymmetry" of these curves as the ratio $(AM-MB)/MB$, taken at one fourth the maximum height, the asymmetry of the delayed curve is 1.1. For the curve obtained by replacing a portion of the

delayed curve by an extrapolation of its left upper part (denoted as (a)) the asymmetry is 0. This latter curve is, for its non-extrapolated part, the sum of a prompt (or slightly delayed) curve and a strongly asymmetric true delayed one. A simple sketch shows that it may therefore be presumed to have an asymmetry larger than that of a prompt curve, especially if the prompt contribution is large. This would mean that the asymmetry of a prompt curve is at most 0.

This is however only an estimate and, with the various graphical uncertainties involved, a conservative upper limit of 0.20 was set for the asymmetry of $P(t)$. It leads (fig.3) to the conclusion that τ ranges between 10 and 22 channels, i.e. $T_{1/2} = 1.01 \pm 0.38$ ns, with the uncertainty being essentially of systematic nature.

It means also that the prompt contribution is rather high ($A/\tau \sim 2$). This is quite in conformity with the general outlook of the experimental curve. But, on the other hand, and even though electron peaks are somehow smeared by a limited momentum resolution ($\sim 3\%$) and inelastic backscattering, it is uneasy to find out the origin of so many prompt coincidences. The functions $P(t)$ corresponding to acceptable values of τ are nearly symmetric at half the maximum and their f.w.h.m is 10 or 11 channels, i.e. ~ 1 ns.

We are in presence of three independent determinations of $T_{1/2}$ (293keV), the first two of which have an unknown but important systematic uncertainty. Weighting these two values by the inverse of their statistical uncertainty leads to $T_{1/2} = 1.2$ ns, which may be considered as one single determination with an approximate systematic uncertainty 0.2 ns (largest distance from either value to the average). Combining this latter value with the third one gives

$$T_{1/2} (293\text{keV}) = 1.1 \pm 0.3 \text{ ns.}$$

The uncertainty is of systematic origin and the confidence level fairly high.

5.2 Lifetime of the 70.7 keV 4^- level

The lifetime of the 70.7 keV level has been studied by $e^- - e^-$ coincidences between the K192 and L70.7 lines (fig.4), here again without any reference prompt curve.

An upper limit for this lifetime can be estimated by using the condition that $P(t)$ should have neither negative values nor secondary maxima (to avoid any computational artefact a negative value was ascertained when $|P(t)|$ reached at least 1% of the maximum value of $P(t)$, the same condition being imposed on the difference between two neighbouring maxima for their identification). If no prompt contribution is present the maximum acceptable τ value is ca. 150 ps. If an eventual prompt contribution with A/τ less than, say, 3 is introduced, this limit increases to 250 ps. Such a loose condition being very likely to be fulfilled, 250ps is an upper bound for τ . A similar result is obtained by the study of a coincidences curve registered after inverting the "start" and "stop" signals (and the direction of the t-axis prior to the numerical calculations). Therefore we may conclude that

$$T_{1/2} (70.7 \text{ keV}) < 180 \text{ ps} .$$

It may be added that an attempt to obtain an upper bound for the lifetime of the 262.7 keV level was done similarly by measuring coincidences between the K92.7 electron line, which feeds directly the level, and the K192 one, which deexcites it (and the reverse coincidence). The delayed coincidence curves were narrow (1ns f.w.h.m.). However a low-intensity tail was present on the K192 line side of the curve. In the absence of any clear explanation for it, no reliable numerical value could be deduced.

5.3 Lifetime of the 225.6 keV 3^+ level

A flat coincidence spectrum was obtained when gating the coincidence setup on the L58.4 and K225.6 and on the L67.8 and K154.8 electron lines. This is in agreement with the level scheme and the finding that the 225.6 keV level is an isomeric state with $T_{1/2} = 0.47 \text{ ms}$ [19].

6. Lifetime measurements in $^{185,187}\text{Pt}$

Levels in $^{185,187}\text{Pt}$ were populated in the EC/β^+ decay [20-22] of $^{185,187}\text{Au}$ obtained by (p, xn) reaction on a Pt-B target. Half-lives are respectively 4.3 and 8.4 min for ^{185}Au and ^{187}Au . Measurements were performed by $e^- - \gamma$ delayed coincidences. A ^{60}Co source provided the prompt reference cur-

ves, the settings remaining unchanged between the registration of the delayed and prompt curves.

6.1 Lifetime of the 260.5 keV $3/2^-$ level in ^{187}Pt

The delayed coincidences curve is shown in fig. 5. The lens of the spectrometer was focused on the K260 line, which appears clearly in the electron spectrum and is free from any admixture with another important electron line. The analysis with the MULPAC program shows no appreciable prompt contribution. The result is $T_{1/2}(260 \text{ keV}) = 163 \pm 6 \text{ ps}$ (statistical uncertainty).

Fig. 5 shows that the best fit obtained, which corresponds to the above mentioned half-life, is more satisfactory for the trailing slope than for the left edge of the curve.

Taking the matter the other way round, one may find, using rel. (2), the prompt curve which would correspond to the experimental delayed curve and to $T_{1/2} = 163 \text{ ps}$. One gets a curve which has a larger f.w.h.m. than the experimental prompt curve (6 channels vs. 4 channels) but which, after convolution (rel. 1), reproduces fairly well the experimental delayed curve. A further investigation shows that the condition that the prompt curve should have no negative values yields $T_{1/2} < 250 \text{ ps}$ and that for $0 < T_{1/2} < 250 \text{ ps}$ the f.w.h.m. of the prompt curve is at least 6 channels. Neither does the introduction of an eventual prompt contribution reduce this width.

The conclusion is that the experimentally produced prompt curve is not exactly suited for the analysis of the delayed curve. This phenomenon is not new but it is clearly demonstrated here. It could be put in relation with drifts produced by the variation of counting rates during a measurement, which are hard to avoid when studying short half-lived nuclei. It means that an uncertainty of systematic origin is present, and it is very difficult to estimate it.

6.2 Lifetime of the 180.8 keV $3/2^-$ level in ^{185}Pt

The L77.6- γ coincidences were used for this determination (fig. 6). The L77.6 conversion lines are intense and rather well separated from other important lines in the direct electron spectrum. The result is

$$T_{1/2}(180.8 \text{ keV}) = 1.68 \pm 0.04 \text{ ns} .$$

The uncertainty is of statistical origin and there is no appreciable prompt contribution. However here again, albeit the fit is satisfactory ($\chi^2=1.04$), the deconvolution analysis shows that the delayed curve corresponds to a prompt curve which has a larger f.w.h.m. than the experimental one (14 channels vs. 8). This determination is presumably less accurate, as the delayed and prompt curves differ strongly, but the same qualitative result is observed on varying the τ and A parameters.

6.3 Lifetime of the 200.8 keV $5/2^-$ level in ^{185}Pt

The 200.8 keV level deexcites mainly through two competing 97.6 keV and 20.0 keV transitions. The L20.0 electron conversion lines are mixed up with the Auger LMN lines, the M20.0 with the K94.8, and the N20.0 with the K97.6. A lifetime measurement was made by (K97.6 + N20.0) - γ coincidences (fig.7). Another one used the M20.0 - γ coincidences. It had a lower counting rate but was not hampered by the K94.8 electrons which are not in coincidence with the 20.0 keV transition. Both measurements are consistent and their weighted average is

$$T_{1/2}(200.8 \text{ keV}) = 728 \pm 20 \text{ ps} .$$

In this case, too, the prompt curves which may be deduced from the experimental delayed curves with any reasonable test value for τ and A have a significantly larger f.w.h.m. than the experimental ones. The systematic occurrence of this phenomenon indicates that it is not related to an accidental drift, due e.g. to a temperature change.

7. Discussion

The measured lifetimes yield electromagnetic transition probabilities, the multipole admixture being already known. No model calculations have been performed. But for odd-odd ^{184}Ir the 67.6 keV and 70.7 keV transitions connect states which have similar configurations in the Two-Quasiparticle-Plus-Rotor model [16]. The reduced M1 and E2 rates (0.06 and 2 Weisskopf units, resp.) for the former transition and the M1 rate (> 0.5 W.u.) for the latter, support this interpretation. In ^{187}Pt the states involved are members of a rotational

band [20] . The E2 transitions are satisfactorily enhanced (9.4 and 20 W.u.) and, as a rough picture predicts, they increase with the transition energy. As to ^{185}Pt , the transition which links the 260.5 keV level with the ground-state has a 5.10^3 Weisskopf M1 hindrance factor. This transition is also undoubtedly abnormally converted [23]. Putting together these two results and comparing them with other ones regarding abnormally converted M1 transitions in ^{175}Lu , ^{181}Ta , ^{203}Tl shows (cf. ref.23) that the correlation between transition retardation and penetration effect in the $A \sim 200$ region is not simple.

8. Conclusion

The method proposed here enables to deduce a lifetime from a delayed coincidence curve when the prompt curve is known only through some general features. As a comment it could be added that the case to which it has been applied is not particularly favourable and that, as already stated, it has been used in a very cautious way. Obviously any other information available about the prompt curve could in principle be utilized. Another conclusion is that, conversely, a supposedly accurate experimental knowledge of the prompt curve is not always a guarantee that no important systematic uncertainty has to be considered. This is of particular relevance for systematic studies of absolute electromagnetic transition rates, or when the lifetime to be measured is close to the lowest value measurable with the device.

We are indebted to Dr. J.Sauvage and Doc. K.Fransson for fruitful comments on the manuscript.

FIGURE CAPTIONS

Fig.1 Electron spectrum of the $^{184}\text{Pt} \longrightarrow ^{184}\text{Ir}$ decay registered with one lens of the magnetic γ -spectrometer. Internal conversion lines are identified by a letter. This spectrum is in good agreement with the high-resolution electron spectrum published in ref.16 .

Fig.2 Time distribution of $e^- - e^-$ delayed coincidences between the L67(start) and the L49 lines in ^{184}Ir , for the determination of the 293.3 keV level lifetime, and partial level scheme of ^{184}Ir . Points A and B are located at one fourth of the maximum of the curve and M is the projection of this maximum on the line AB. Random coincidences (4 counts) have been subtracted. The time calibration is 91 ps/channel.

Fig.3 Value of the asymmetry of the prompt curve as a function of A/τ and τ for the delayed curve of fig.2 (after reversing the t-axis). Contours represent equal values of the asymmetry. The hatched area is excluded by the condition that $P(t)$ should have neither negative values nor secondary maxima (cf. sect. 5.1).

Fig.4 Time distribution of the L70.7(start)-K192 coincidences in ^{184}Ir . No background has been subtracted.

Fig.5 Time distribution of the K260(start)- γ coincidences in ^{187}Pt . The best fit (dashed line) is obtained with virtually no prompt contribution.

Fig.6 Time distribution of the L77.6(start)- γ coincidences in ^{185}Pt . For clarity the prompt curve has been shifted one decade downward ($\times 0.1$). The dashed curve represents the best fit, which is reached when no prompt contribution is present.

Fig.7 Time distribution of the (K97.6 + N20.0)(start)- γ coincidences in ^{185}Pt . The best fit corresponds to $A/\tau \sim 0.5$.

REFERENCES

- 1) R.E.Bell, R.L.Graham and H.E.Petch, *Can.J.Phys.* 30 (1952) 35
- 2) J.Lindskog, E.Bashandy and T.R.Gerholm, *Nucl.Phys.* 16 (1960) 175
- 3) M.C.Abreu, J.P.Ribeiro and F.B.Gil, *Portgal.Phys.* 11 (1980) 1
- 4) W.Andrejtscheff, M.Senba, N.Tsoupas and Z.Z.Ding,
Nucl.Instr.Meth. 204 (1982) 123
- 5) P.Petkov et al., *Nucl.Phys.* A554 (1993) 189
- 6) L.K.Kostov et al., *Z.Phys.* A348 (1994) 79
- 7) M.Büscher et al., *Phys.Rev.* C41 (1990) 1115
- 8) M.Liang, *Diss.Univ.Köln, Forschungszentrum Jülich Rep.* n.2663
- 9) M.Hellström et al., *Phys.Rev.* C47 (1993) 545 and ref. therein;
N.V.Zamfir et al., *Phys.Rev.* C51 (1995) 98
- 10) C.Bargholtz and K.Fransson, *Nucl.Instr.Meth.* 158 (1979) 515
- 11) L.Boström, B.Olsen, W.Schneider and E.Matthias,
Nucl.Instr.Meth. 44 (1966) 61
- 12) T.D.Newton, *Phys.Rev.* 78 (1950) 490
- 13) R.Théodor, *Initiation à l'analyse numérique*, Masson, Paris (1989)
- 14) P.Paris et al., *Nucl. Instr.Meth.* 186 (1981) 91; J.C.Putaux et al.,
Nucl.Instr.Meth. 186 (1991) 321
- 15) T.R.Gerholm and J.Lindskog, *Ark.Fys.* 24 (1963) 171
- 16) A.Ben Braham et al., *Nucl.Phys.* A482 (1988) 553
- 17) R.B.Firestone, *Nucl.Data Sheets* 58 (1989) 243
- 18) C.Bargholtz, *Nucl.Instr.Meth.* 120 (1974) 121; *Univ. of Stockholm Inst.
of Phys. Rep.* USIP 74-08
- 19) A.J.Kreiner et al., *Nucl.Phys.* A489 (1988) 525
- 20) B.Roussièrè et al., *Nucl.Phys.* A438 (1985) 93
- 21) B.Roussièrè et al., *Nucl.Phys.* A485 (1988) 111;
E.Browne, *Nucl.Data Sheets* 58 (1989) 441
- 22) R.B.Firestone, *Nucl.Data Sheets* 62 (1991) 159
- 23) B.Roussièrè et al., *Nucl.Phys.* A548 (1992) 227

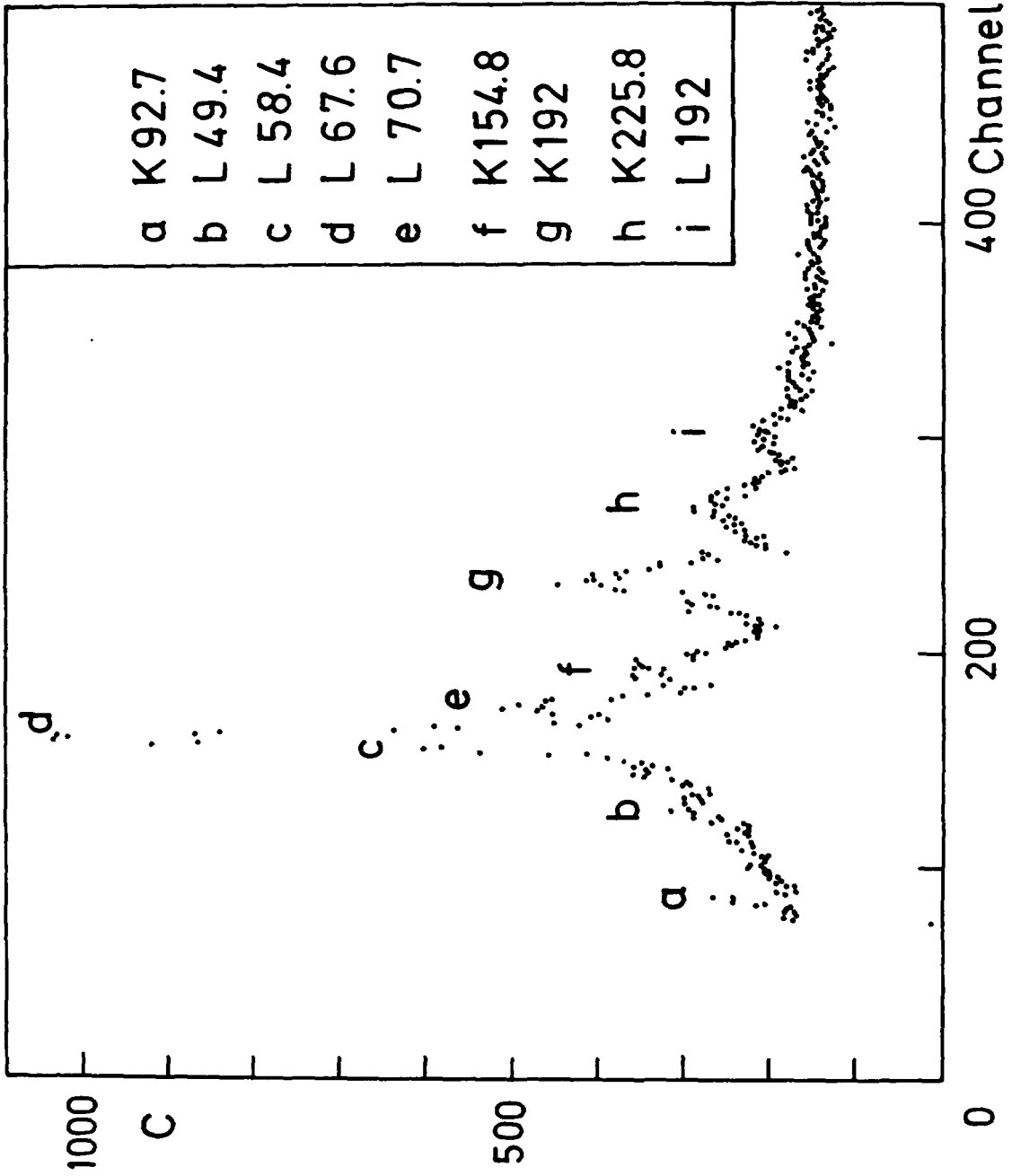


fig. 1

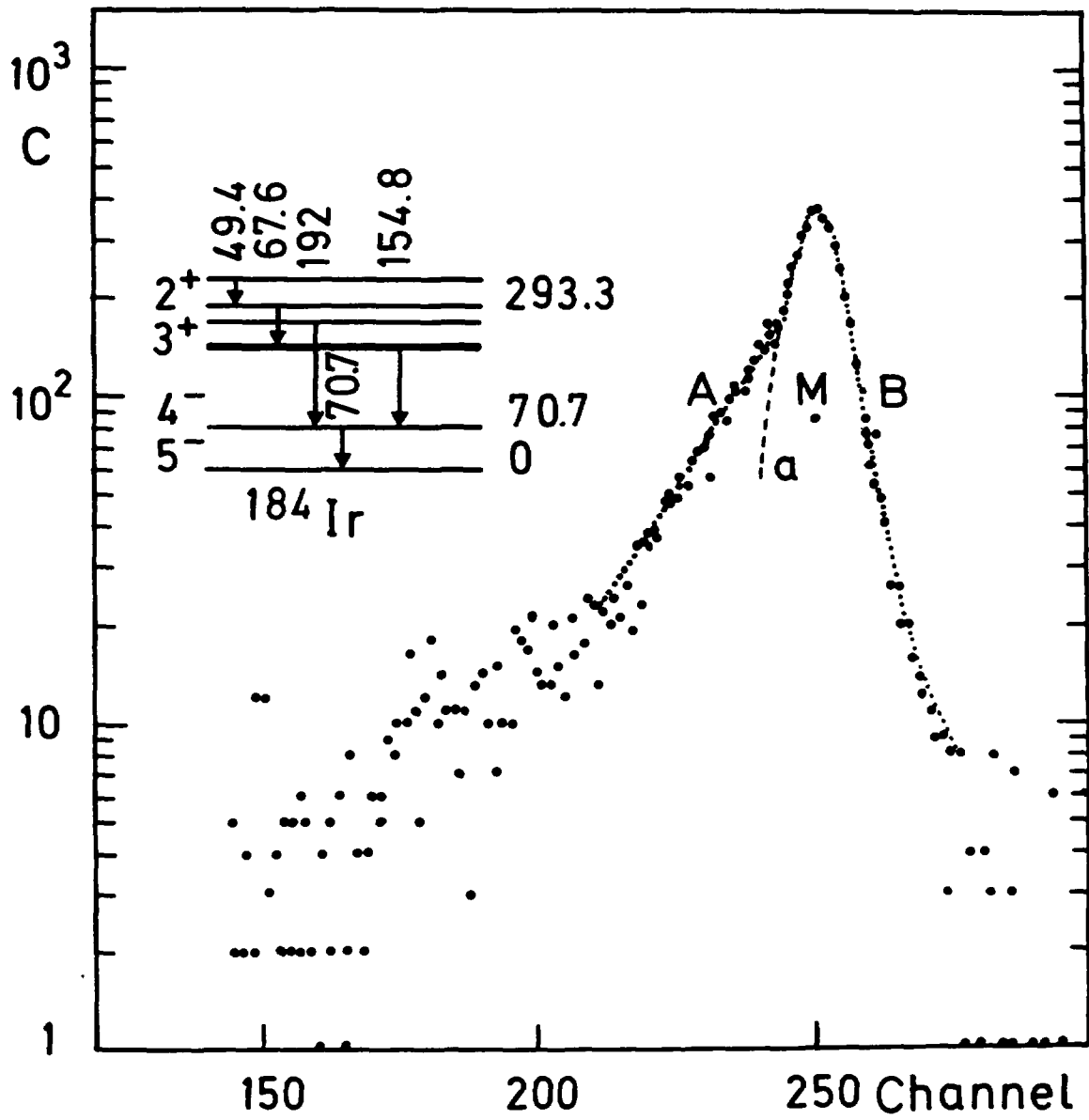


fig. 2

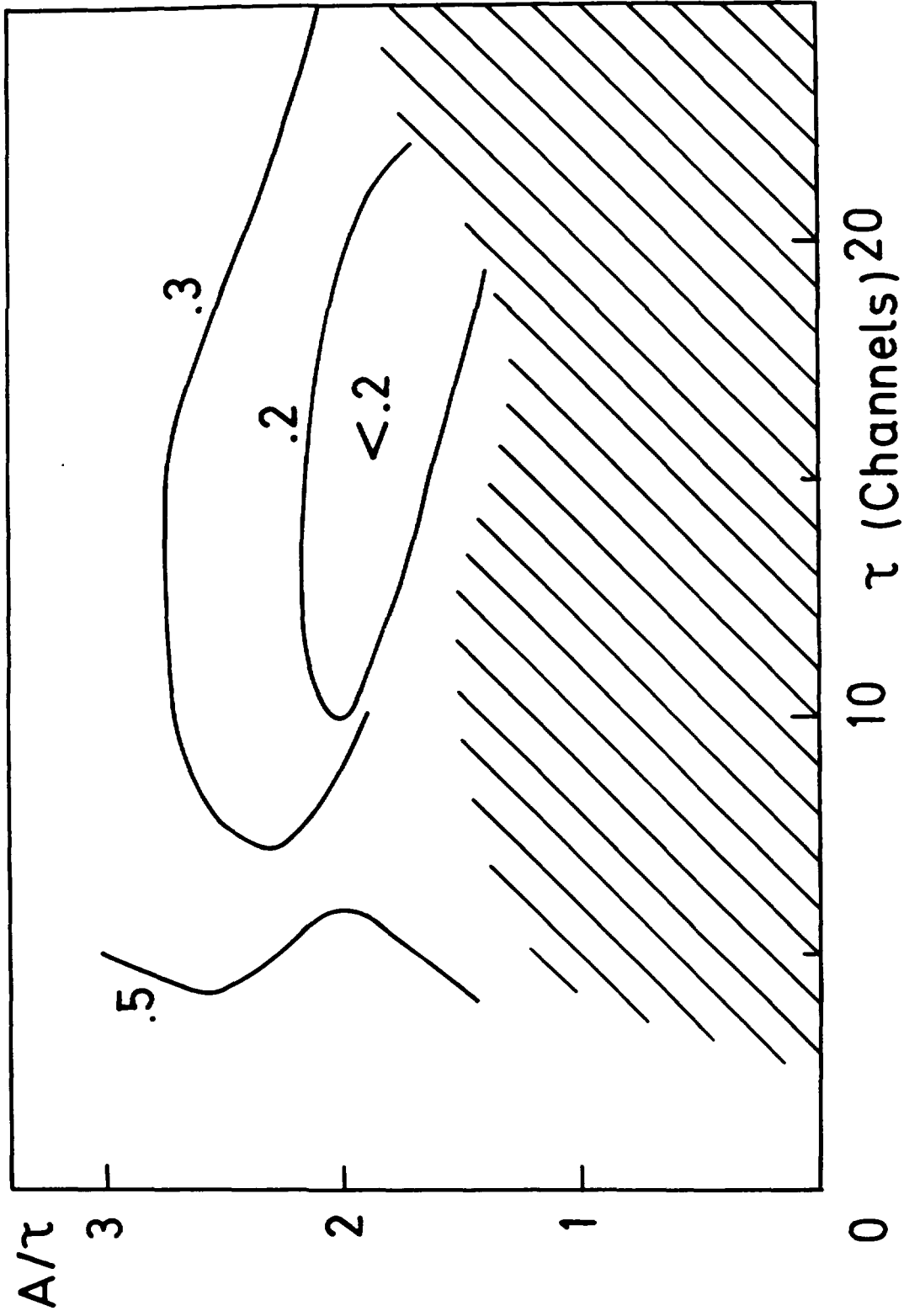


fig. 3

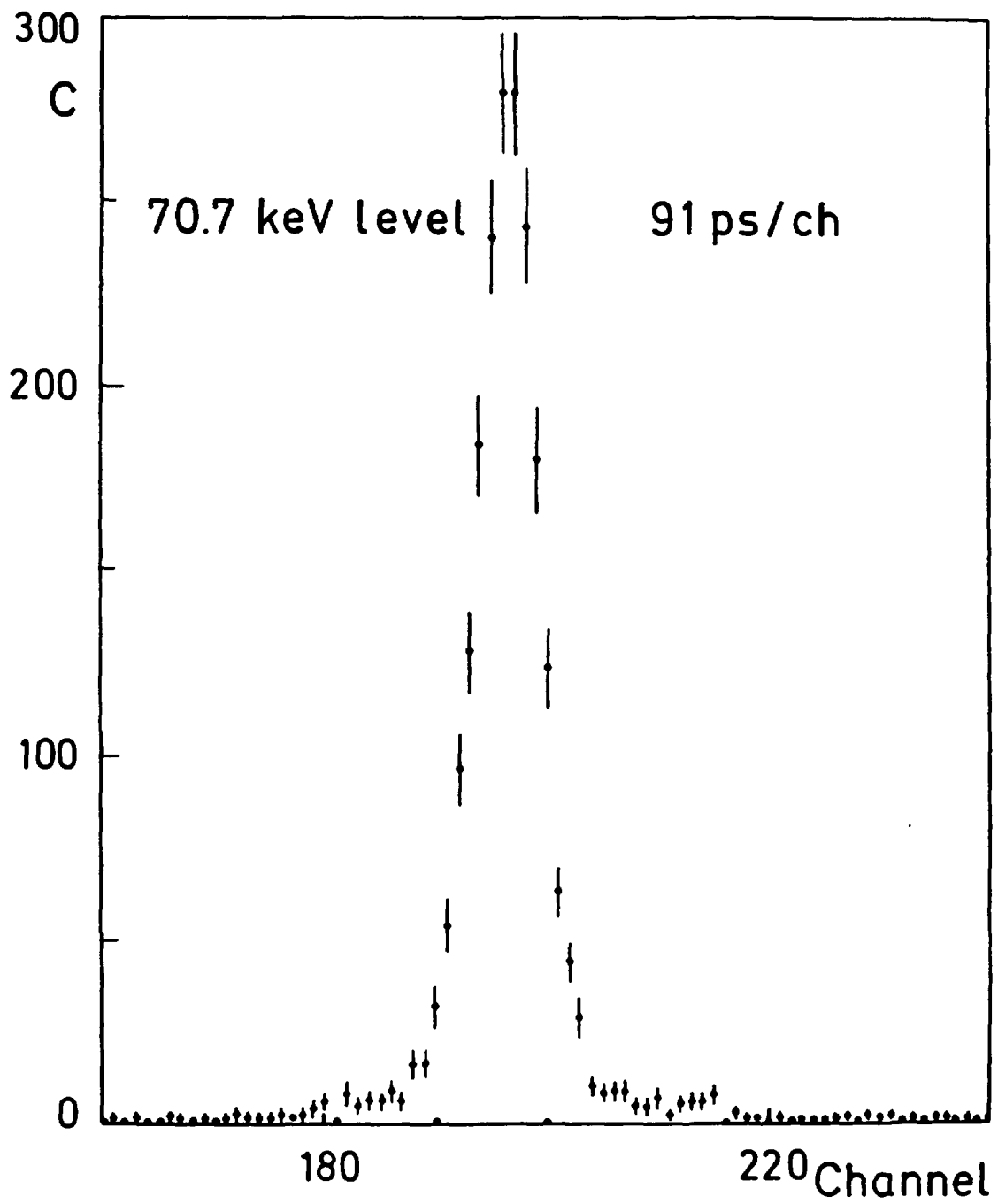


fig. 4

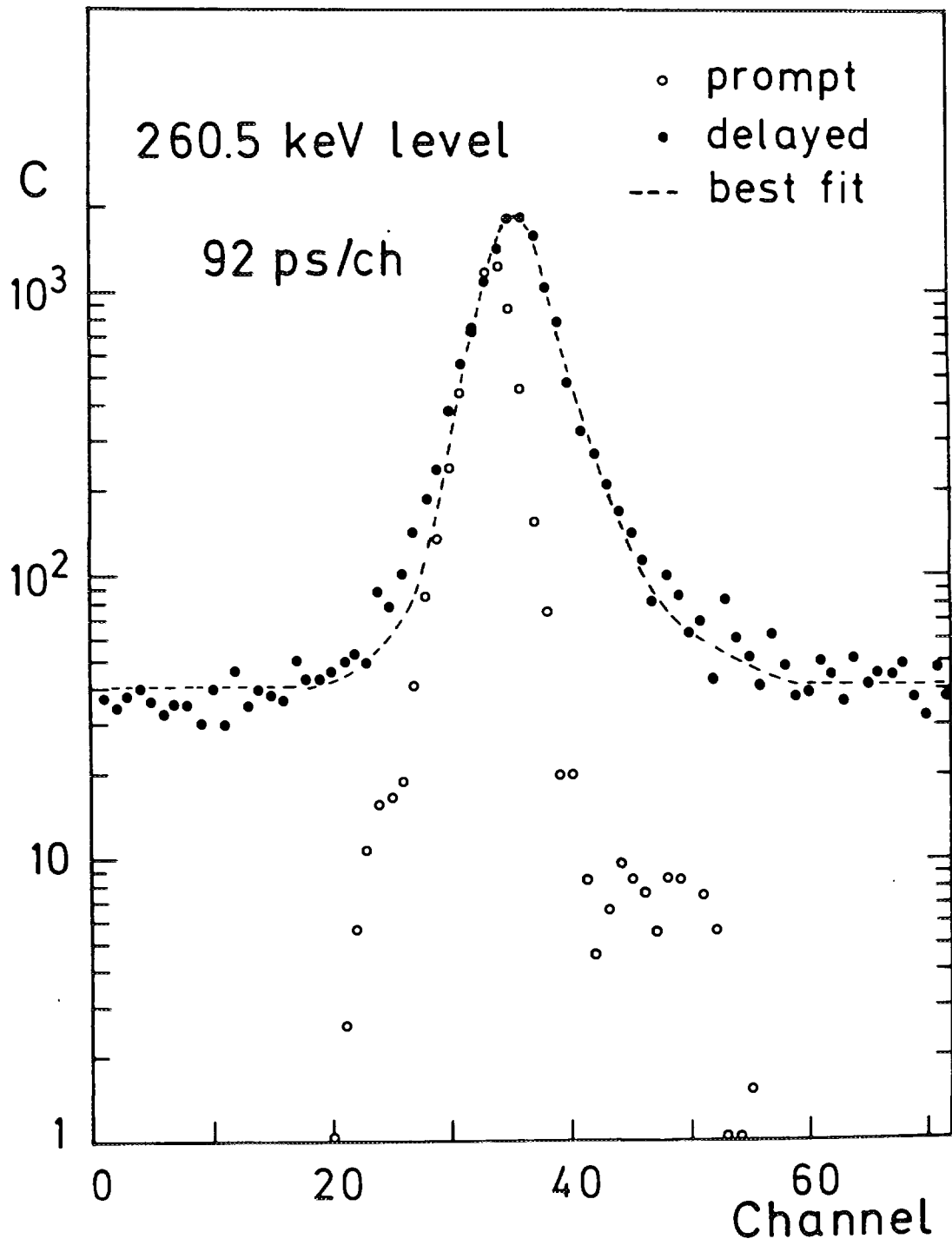


fig. 5

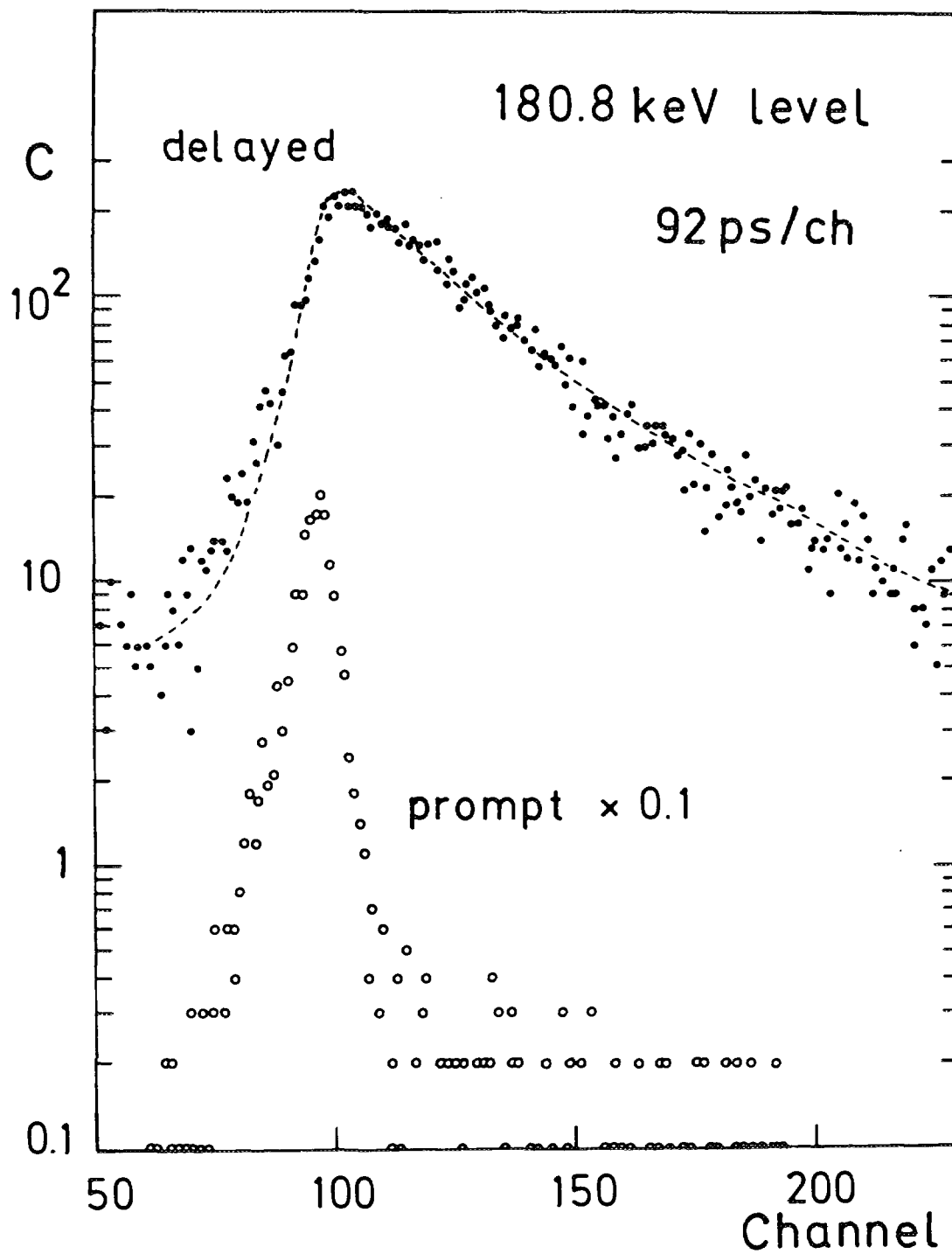


fig. 6

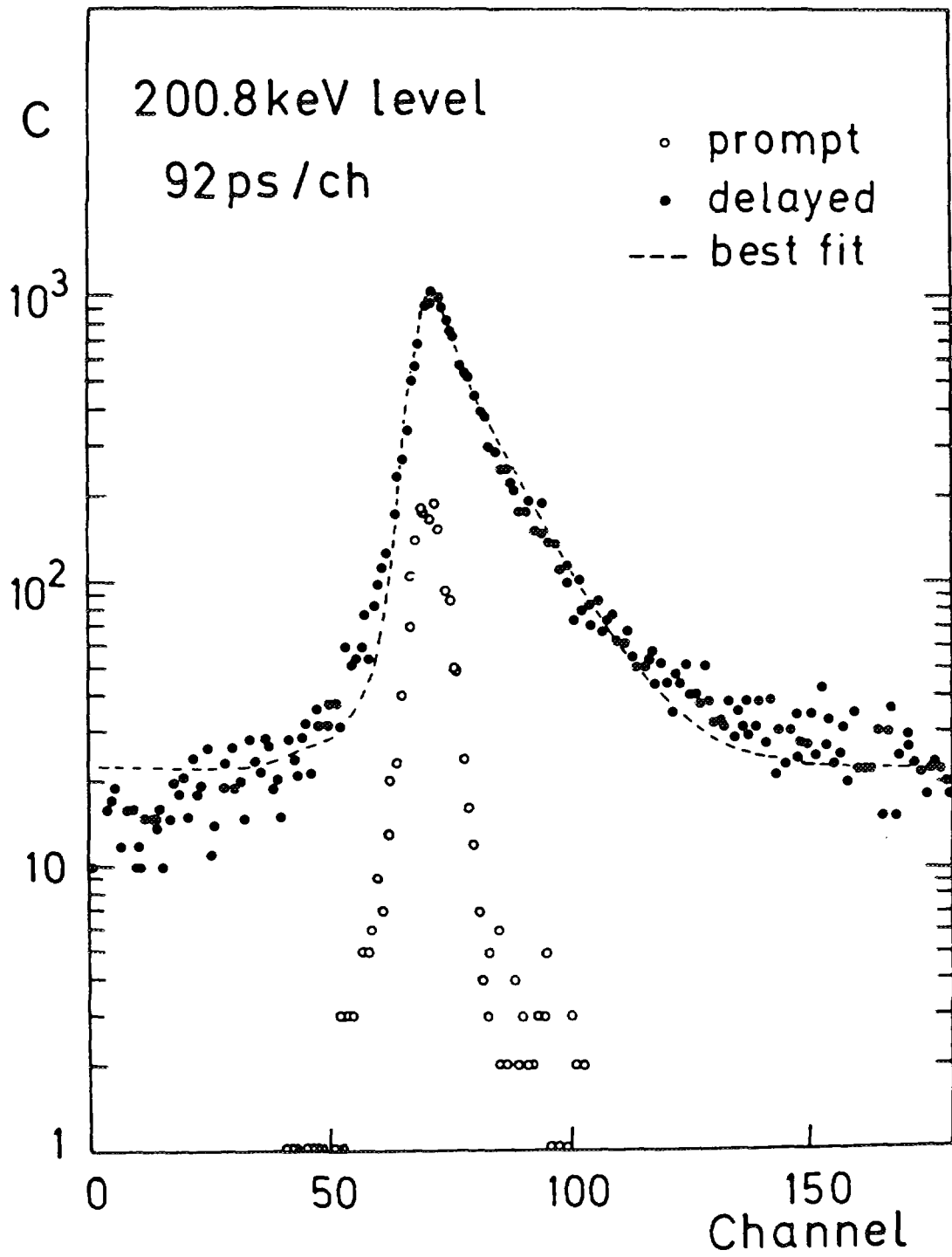


fig. 7